Effect of Molar Mass and Regioregularity on the Photovoltaic Properties of a Reduced Bandgap Phenyl-Substituted Polythiophene

Farid Ouhib,[1] Guillaume Dupuis,[1] Rémi de Bettignies,[2] Séverine Bailly,[2] Abdel Khoukh,[3] Hervé Martinez,[4] Jacques Desbrières,[1] Roger C. Hiorns,[3] Christine Dagron-Lartigau[1]

[1]IPREM (EPCP) UMR 5254, Université de Pau et des Pays de l'Adour, 2 avenue President Angot, 64053 Pau, France
[2]INES-RDI DRT/LITEN/DTS/LCS Savoie Technolac BP 332, 50 avenue du lac Léman, 73377 Le Bourget du Lac, France
[3]CNRS, IPREM (EPCP) UMR 5254, 2 avenue President Angot, 64053 Pau, France
[4]IPREM (ECP) UMR 5254, Université de Pau et des Pays de l'Adour, 2 avenue President Angot, 64053 Pau, France
Correspondence to: C. Dagron-Lartigau (E-mail: christine.dagron-lartigau@univ-pau.fr)

Received 20 September 2011; accepted 24 January 2012; published online 23 February 2012
DOI: 10.1002/pola.25970

ABSTRACT: Among the numerous reduced bandgap polymers currently being developed, poly[3-(4-octylphenyl)thiophene)]s (POPT) may present attractive properties for organic solar cells due to its facile preparation and improved absorption with respect to poly(3-hexylthiophene). This article appraises methods of preparation, including the use of diphenyl ether as a reaction medium, and discusses the effects of variations in molar masses, from about 3200 to 65,000 g mol^{-1} and regioregularity on its optoelectronic properties. The photovoltaic properties of POPT with [6,6]-phenyl C_{61} butyric acid methyl ester (PCBM) in bulk heterojunction devices are also discussed in the light of morphological variations, as indicated by atomic force microscopy characterizations. With an initial screening of conditions, namely POPT:PCBM ratios and deposition solvent, a power conversion efficiency of 1.58% was obtained using a relatively high molar mass POPT sample. © 2012 Wiley Periodicals, Inc. J Polym Sci Part A: Polym Chem 50: 1953–1966, 2012

KEYWORDS: chain growth polymerization polythiophenes; conjugated polymers; Grignard metathesis chain growth polymerizations; [6,6]-phenyl C_{61} butyric acid methyl ester (PCBM); photovoltaic devices; poly[3-(4-octylphenyl)thiophene]

INTRODUCTION Their low cost and ease of processing have pushed polymer-based solar cells organic photovoltaics (OPVs) to the forefront of the search for energy sources that do not pollute the environment with CO_2.[1–3] It is expected that as soon as 10 year, 10% efficiency OPVs can be mass-produced, there will be a paradigm shift in the market place.[4,5]

In OPVs, such as that in Figure 1, the dominant process is of light absorption by the polymer to form excitons that can move around 10 nm, and on meeting an interface with an acceptor molecule, fast electron transfer results in a positively charged polymer and a negatively charged acceptor.[6–8] The conduction of these charges to the respective electrodes gives electricity. The absorption qualities of the materials, along with the positions of their electronic bands, and the nanomorphology of the materials in the active layer, impinge strongly on the OPV qualities.[9,10] A considerable wealth of knowledge has been gained through the use of an active-layer based on poly(3-hexylthiophene) (P3HT) and [6,6]-phenyl C_{61} butyric acid methyl ester (PCBM), which have shown efficiencies of around 5%.[11] More recently, great gains have been made through the use of the so-called low bandgap polymers which display increased absorptions in the about 600–900 nm range,[12–15] such that OPV efficiencies of around 8% are now feasible.[16,17] However, these materials remain relatively complex to prepare, and an objective remains to find new materials that can deliver the requisite properties at low costs. Polythiophene-based materials are of interest due to their ease of preparation and the high degree of control over polymer molar masses afforded by the Grignard metathesis (GRIM) polymerization route,[18–23] which can be facilely performed at room temperature.[24]

Modification of the position-3 in the thiophene group is relatively facile and leads to considerable changes in optoelectronic properties. For example, Oshimizu et al. introduced phenyl or pyridinyl groups into the side-chains and found that the former gave rise to more crystalline polymers. Indeed, both showed a decrease in HOMO and bandgaps (E_g) with respect to P3HT, although the phenyl-derivative showed a greater decrease due to the increased π-conjugation.[25] Reduced bandgaps and improved hole-mobilities have also been obtained through introducing, for example, conjugated thiophene-2,5-diyl pendent moieties or crosslinking

Additional Supporting Information may be found in the online version of this article.

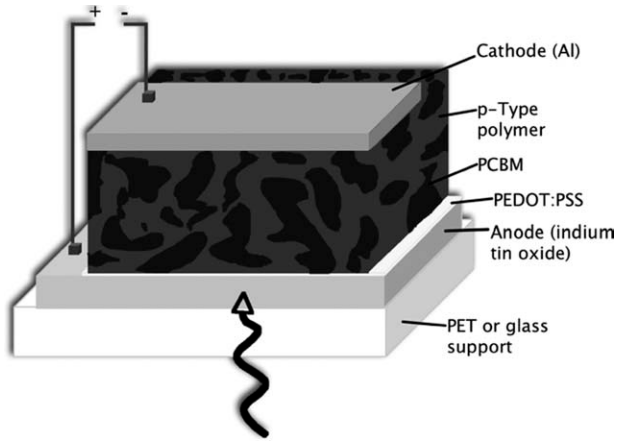

FIGURE 1 "Normal" OPV device structure.

agents.[26–29] Inter-chain branches have similarly been explored.[30] These works have demonstrated that the optoelectronic properties and the way in which the materials self-organize is exceptionally sensitive to the nature and degree of side-chain modification. And while the work on the so-called "double-cable"[31] polythiophenes was also susceptible to disorganizing the polythiophene backbone, it did demonstrate the exceptional degree of modifications that can be made at the 3-thiophene position, notably through the introduction of fullerene[32] and PCBM-like moieties.[33]

Poly[3-(4-octylphenyl)thiophene] (POPT) was first prepared in 1992 as a variation to the already well-known poly(3-alkylthiophene)s (P3AT). It was thought that the introduction of a phenyl ring into the side chains would enhance conjugation and thermal stability.[34] The initial reactions leading to POPT were based on the facile oxidation polymerization of 3-(4-octylphenyl)thiophene using Fe^{3+} (Fig. 2).[35] Samples suffered though from relatively low-molecular weights (up to around 23,000 g mol^{-1}) and high dispersities. And although the properties of POPT, such as its relatively high value of λ_{max} and good thermal stability, make it of interest for use in photovoltaic cells. Previous results, showed 1.9% (simulated solar spectrum at 77 mW cm^{-2}) was obtained on a bilayer device with a cyano poly(*p*-phenylene vinylene) derivative acceptor.[36] The same acceptor with POPT in a bulk heterojunction resulted in average power conversion efficiencies (PCEs) of about 2%.[37] Devices based on blends of POPT with a vinazene derivative yielded to an average PCE of 1.4%, whereas 1.1% was obtained with blends of P3HT with this acceptor.[38] More recently, the effect of side-chain densities on packing structure and photovoltaic performances with PCBM as an acceptor was studied on POPT and POPT derivatives with two or three thiophene spacer units. Best results were achieved (2.77%) with the latter.[39]

It is evident that the poor control over POPT molar masses has hampered its use in devices. More recent, albeit initial, work showed that it was possible to prepare relatively high molar masses of POPT using the GRIM route,[40] and furthermore, that POPT can be combined with P3HT as block copolymers using this method.[41] We therefore decided to explore the control over the GRIM-based polymerization leading to POPT and furthermore study the effect of its molar mass and regioregularity on its photovoltaic properties. A series of comparable reactions were thus performed using the oxidative polymerization of 3-(4-octylphenyl)thiophene (**3**) with Fe^{3+}, and the GRIM polymerization of 2,5-dibromo-3-(4-octylphenyl)thiophene (**4**) in tetrahydrofuran (THF) or in diphenyl ether (DPE), as described in Figure 2. The various POPTs were then compared with respect to their molar mass distributions and their thermal, optical, and photovoltaic properties. To better understand the effects of thermal annealing, deposition solvent, and POPT:PCBM ratios on photovoltaic behaviors, a study of the morphology of the active layer was performed using atomic force microscopy (AFM).

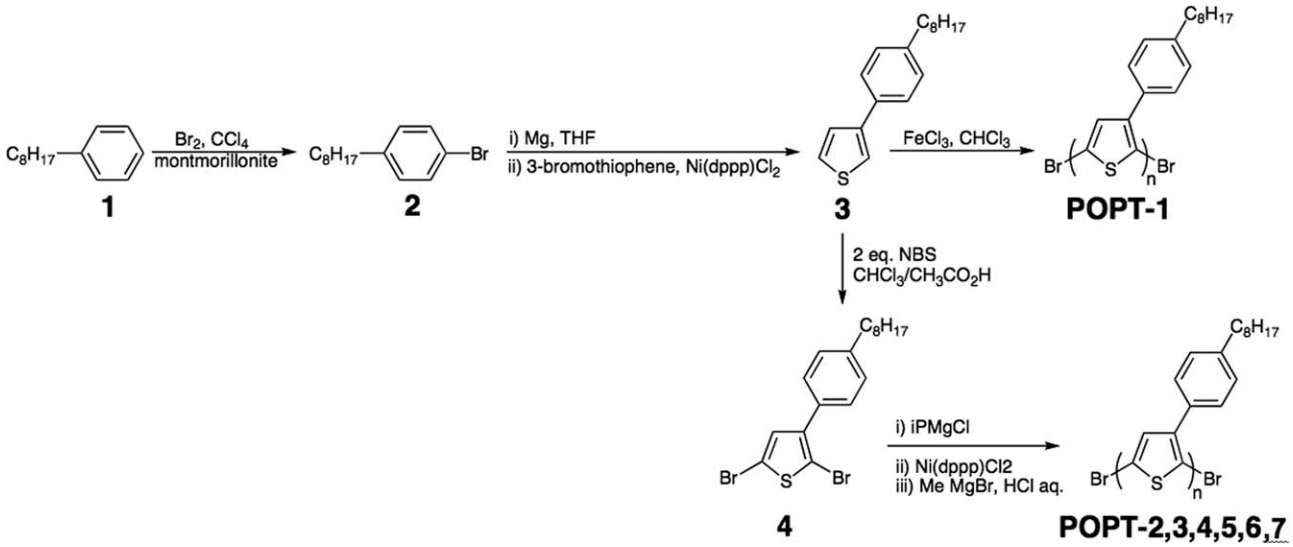

FIGURE 2 Synthetic routes to POPTs.

EXPERIMENTAL

Materials

Chemicals were obtained from Aldrich (France) and used as received. Solvents (Baker, France) were distilled from over standard drying agents under dry nitrogen. DPE was dried over CaH_2 under nitrogen and filtered via a syringe equipped with a Whatman® type "B" glass filter before use. All reactions were performed under dry nitrogen.

Instrumentation

^{13}C (100 MHz) and ^{1}H (400 MHz) NMR spectra were recorded on a Bruker® Avance 400 spectrometer. Polymer molecular weights were estimated against polystyrene (PS) standards using gel permeation chromatography (GPC) as detailed in ref. 41. Ultraviolet (UV)-visible absorption spectra were recorded on a Shimadzu UV-21021PC spectrometer using solutions or spin-coated films. Differential Scanning Calorimetry (DSC) was performed using a TA Instruments DSC Q100 with samples on their second thermal run and at 10 °C min^{-1}. Thermal Gravimetric Analyses (TGA) were performed using a TA Instruments TGA Q50 at 10 °C min^{-1} and under air. AFM imaging was performed with a Veeco® (now Bruker®) MultiMode Scanning Probe Microscope with a Nanoscope IIIA and Quadrex controller. A preliminary study optimizing the working conditions found that "contact" mode resulted in poorer topographic definition than "tapping" mode. Moreover, various tips were tested to find a good compromise between a low radius of curvature, permitting a high resolution and sufficient inflexibility for the weakest possible abrasion during scanning. Taking into account these preliminary results, all AFM images were acquired in intermittent contact mode (tapping) to obtain topographic (with a scanning frequency from 0.4 to 0.8 Hz), phase and deflection (error signal) images using a MPP-11100 Veeco probe (quoted probe radius of curvature less than 10 nm). Phosphorus (*n*) doped Si with a force of 20–80 N m^{-1} at a resonance frequency of about 290 kHz was used. This instrument was used in a glove box under dried argon atmosphere. To complete the quantitative analysis, the size of plate sides was evaluated by taking into account 30 measurements with a typical deviation of 1 nm.

Preparation and characterization of the solar cell devices were performed at the French National Institute for Solar Energy (INES, Chambéry). The current–voltage characteristics and PCE values of the solar cells were measured in an inert gas atmosphere via a computer-controlled Keithley SMU 2400 unit using 100 mW cm^{-2} AM1.5 simulated white light from a Steuernagel Solar Constant 575 simulator. A mono-crystalline silicon solar cell, calibrated at the Fraunhofer-Institut für Solare Energiesysteme (Freiburg, Germany) was used as the reference cell to confirm stabilization of the 100 mW cm^{-2} illumination. Devices (28 mm^2 active surface) were prepared as detailed in ref. 41 with the exception that the active POPT-*blend*-PCBM (1:1 by weight ratio) layer was deposited by spin-coating from an anhydrous chlorobenzene solution (10 mg mL^{-1}) under dry nitrogen to obtain films about 40 nm thick. Annealing, where performed, was for 5 min. Following drying under reduced pressure at 2×10^{-7} mbar for 1 h, devices were completed by deposition of LiF/Al (0.8 and 100 nm, respectively) cathode through a shadow mask with 6 mm diameter openings at about 2×10^{-7} mbar. Cell illumination was through the ITO side. η of the devices was calculated using eqs 1 and 2:

$$\eta = \mathrm{FF}\frac{V_{oc}J_{sc}}{P_{in}} \quad (1)$$

$$\mathrm{FF} = \frac{V_{max}J_{max}}{V_{oc}J_{sc}}, \quad (2)$$

where P_{in} is the power of incident light and V_{max} and J_{max} represent the voltage and current densities at the maximum power point, respectively.

Syntheses

Poly[3-(4-octylphenyl)thiophene] via $FeCl_3$ (POPT1)

To **3** (5.51 mmol) dissolved in chloroform (30 mL) was added a suspension of $FeCl_3$ (27.57 mmol) in chloroform (70 mL) over a period of 4 h. The final concentration of monomers and $FeCl_3$ was 0.05 and 0.27 M, respectively. The reaction mixture was stirred at room temperature for 20 h and poured into methanol (700 mL). The precipitate was filtered off, washed with methanol, dissolved in chloroform, and dedoped with ammonia solution (1 M, aq.). The mixture was stirred for 24 h, and the water phase replaced with fresh ammonia solution. This procedure was repeated another four times, and then the chloroform solution was washed twice with ethylenediamine tetraacetic acid (0.05 M, aq.). The chloroform solution was washed with water and poured into methanol (400 mL). The precipitated polymer was Soxhlet washed with diethyl ether and recovered with chloroform. After evaporation of the solvent, the polymer labeled POPT-1 was dried under reduced pressure at 70 °C for 24 h and 1 h at 130 °C (yield 46.6%). ^{1}H NMR ($C_2D_2Cl_4$, 100 °C): 7.33 (2 H, dd, $J_3 = 8$ Hz), 7.25 (2 H, dd, $J_3 = 8$ Hz), 6.9 (1 H, s), 2.73 (2 H, t, $J_3 = 7.29$ Hz), 1.75 (2H, m), 1.40 (10H, m), and 0.99 (3 H, t, $J_3 = 7.2$ Hz). ^{13}C NMR ($C_2D_2Cl_4$, 100 °C): 143.1, 140.1, 134.8, 133.6, 131.4, 130.3, 129.5, 128.9, 36.1, 32.3, 31.5, 29.8, 29.7, 29.6, 23, and 14.4 ppm. Molecular weights for this polymer and other details are given in Table 1.

Poly[3-(4-octylphenyl)thiophene] using Ni(dppp)Cl_2 in THF (POPT2)

In a 100 mL three-necked round bottomed flask, **4** (2.32 mmol) was dissolved in THF (12 mL). Isopropylmagnesium chloride (iPMgCl) in THF (2 M, 2.32 mmol) was added, and the mixture was stirred at 40 °C for 2 h. Ni(dppp)Cl_2 (0.046 mmol; ratio Ni:monomer was 1:50, respectively) was added in one portion, and the reaction mixture was stirred at 40 °C for an additional 60 h. The polymerization was terminated by the addition of methylmagnesium chloride in THF (3 M, 0.01 mmol) and stirring for 1 h. The polymer was precipitated in methanol, then Soxhlet washed with diethyl ether (to remove unreacted monomer, small oligomers, and Ni salts), and recovered with chloroform. Removal of the solvent and drying under reduced pressure at 70 °C for 24 h gave a near negligible yield of POPT2. ^{1}H NMR ($CDCl_3$,

TABLE 1 POPT Samples and their Primary Characteristics

Polymer (synthesis)	[Ni]/[M]	M_W (g mol^{-1})[a]	Đ	Regioregularity (%)[b]	λ_{max} (nm) in Solution	λ_{max} (nm) POPT Film[c]	λ_{max} (nm) POPT-*blend*-PCBM Film[c]	Optical E_g (eV)[d]
POPT1 ($FeCl_3$)	–	53,000	2.4	94	477	560, **598**, 652	568, **614,** 670	1.76
POPT2 (GRIM)	50	3,200	1.2	Low	–	–	–	–
POPT3 (GRIM, fraction THF)	50	11,900	1.4	90	472	**547,** 580, 640	**486**	1.80
POPT4 (GRIM, fraction $CHCl_3$)	50	49,000	1.5	95	470	560, **600**, 656	568, **614,** 675	1.74
POPT5 (GRIM, fraction C_6H_5Cl)	50	65,000	1.5	91	473	557, **598**, 656	570, **618**, 678	1.74
POPT6 (not fractionated)	500	50,000	1.6	~100	470	563, **606**, 664	569, **614**, 672	1.76
POPT7 (GRIM, fraction $CHCl_3$)	500	39,000	1.7	95	478	**550**, 588, 642	569, **614**, 672	1.76

[a] Determined by GPC against polystyrene standards.
[b] Calculated from ^{1}H NMR.
[c] UV-visible absorption maximum wavelength obtained on annealed (120 °C for 5 min) spin-coated films.
[d] The optical bandgap was obtained from the formula $E_g = 1240/\lambda_{onset}$, where λ_{onset} is the onset value of absorption spectrum of POPT films at high wavelengths.

ambient): 7.03 (5 H, m), 2.60 (2 H, m), 1.65 (2 H, m), 1.31 (10 H, m), and 0.91 (3 H, t) ppm.

Poly[3-(4-octylphenyl)thiophene] using Ni(dppp)Cl_2 in DPE (POPT3 to POPT5)

The following is a representative method. In a 250 mL three-necked round bottomed flask, **4** (5.02 mmol) was dissolved in DPE (50 mL). iPrMgCl in THF (2 M, 5.02 mmol) was added, and the mixture was stirred at 40 °C for 2 h. Ni(dppp)Cl_2 (0.1 mmol, ratio Ni:monomer was 1:50, respectively) was added in one portion, and the reaction mixture was stirred at 60 °C for an additional 60 h. The polymerization was terminated by the addition of CH_3MgBr in THF (3 M, 0.03 mmol) and stirring for 1 h. Precipitation in methanol yielded the crude polymer. This was washed in a Soxhlet with diethyl ether and then sequentially with THF, $CHCl_3$, and chlorobenzene, to give POPT3 (220 mg, 16%), POPT4 (295 mg, 21%), and POPT5 (275 mg, 20%), respectively. Yields given are following sample drying at 70 °C for 24 h and then at 130 °C for 1 h.

Poly[3-(4-octylphenyl)thiophene] using Ni(dppp)Cl_2 in DPE (POPT6)

An additional reaction using a ratio 4 (2.155 mmol) to Ni(dppp)Cl_2 (4.31×10^{-3} mmol) of 500 in DPE (40 mL) was performed. All other reagents were used at the same ratios with respect to the monomer as in the representative method, but the temperature for polymerization was kept at 40 °C. The obtained polymer was washed with diethyl ether in a Soxhlet and recovered with dichlorobenzene yielded POPT6 (150 mg, 25%). POPT3, POPT4, POPT5, and POPT6 gave NMR ^{1}H and ^{13}C spectra as that of POPT1 with variations in sizes of minor signals.

Poly[3-(4-octylphenyl)thiophene] using Ni(dppp)Cl_2 in DPE (POPT7)

The same procedure as for POPT3 to POPT5, in particular for reaction temperatures was used. The only difference is the monomer:Ni ratio of 500. The sample of POPT7 was recovered after fractionation from chloroform.

RESULTS AND DISCUSSION

Monomer and Polymer Syntheses

Figure 2 presents the routes to monomers and polymers. The bromination of octylbenzene to yield 1-bromo-4-octylbenzene (**2**) was performed in the presence of montmorillonite clay[42] rather than the more habitually used Fe.[43] This resulted in a slight improvement in both yield and selectivity, even if **2** was contaminated with about 14% of the isomer 1-bromo-2-octylbenzene. However, on addition of **2** to 3-bromothiophene, using a well-established route in the presence of Ni(dppp)Cl,[44,45] the resulting 3-(4-octylphenyl)thiophene (**3**) was found to be *quasi*-pure. The isomer was in effect excluded from the reaction with 3-bromothiophene, perhaps by steric effects. This is important to note as variations in the position of the group adjunct to the phenyl ring strongly impact on the polymer properties.[43] The preparation of the brominated monomer, 2,5-dibromo-3-(4-octylphenyl)thiophene (**4**) was found to be facile using *N*-bromosuccinimide, and the reaction gave yields comparable with those found for alkylated thiophenes.[22]

Molar Masses and Regioregularities

Polymer molar mass affects OPV properties at several levels: first, the length of the polymer must be great enough to avoid electron confinement effects that limit absorption;[46] second, high molar mass polymers tend to form fibrillar structures across the composite that increase π-π interactions between adjacent chains and enhance charge conduction through the device, while medium and lower molar mass polymers can enhance interactions with the acceptor molecules; and third, higher molar mass materials generally require greater annealing temperatures to attain ordered structures.[47]

POPTs prepared using oxidative polymerizations (POPT1) and GRIM routes (POPT2–7) have molar masses detailed in Table 1. The values were obtained against PS standards using a GPC with THF as eluant and therefore should be treated with caution; a closely related polymer, P3HT, is known to have lower molar masses than those indicated by

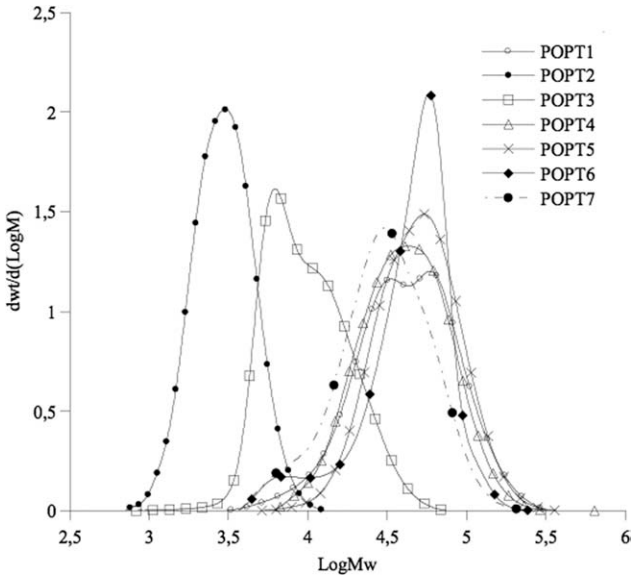

FIGURE 3 GPC chromatograms of POPT samples 1 to 7 (THF, UV-254 nm).

GPC under similar circumstances.[48] Nevertheless, POPT1 was found to have M_w = 53,000 g mol^{-1}, a bimodal distribution (see Fig. 3), and a high dispersity (Đ = M_w/M_n) of 2.4; values that are in accordance with those described in the literature for the oxidative polymerization.[35]

Given the known nature of the mechanism,[18] the GRIM chain-growth polymerization was expected to deliver POPTs higher regioregularity and molar masses. POPT2 was prepared with a ratio monomer to Ni 50:1 and was therefore expected to have a degree of polymerization of around 50 units. POPT2 had a surprisingly low molar mass of around 3200 g mol^{-1}. Given the probable difference in hydrodynamic volumes for PS and POPT, the average number degree of polymerization of POPT2 was at most around 10, quite below that expected. POPT2 was most likely poorly solvated by THF and precipitated out from the reaction mixture before the full chain length could be reached. The use of DPE as a solvent in the place of THF and for a same ratio monomer to Ni (50:1) made it possible to obtain a crude polymer sample with a much higher molar mass, indeed so high that it was only partly soluble in the GPC solvent THF. To obtain a rough estimate to the molar mass of this crude polymer, an attempt to modify it using bromination (with the most likely effect of causing steric-disruption of aggregates) with a small quantity of Br_2 in CCl_4 was attempted. GPC analysis of this modified polymer indicated M_w = 21,000 g mol^{-1} and Đ = 2.1. The high dispersity was probably due to the uncontrolled nature of the polymerization, probably either due to its rapidity with respect to the period of initiation, or precipitation. Either way, this result was a definite improvement on those obtained using THF. To obtain a selection of resolvable samples, the crude polymer was sequentially fractionated in a Soxhlet with solvents of increasing solvating power. Thus, THF (POPT3, 27% w/w of the crude polymer), $CHCl_3$ (POPT4, ca. 38% w/w), and chlorobenzene (POPT5, 35% w/w) soluble fractions were prepared. As POPT4 and POPT5 were only slightly soluble in THF, they were slowly transferred from chlorobenzene into warm THF (GPC eluent) just before GPC analysis. Another GRIM polymerization was realized in DPE at 40 °C with a monomer:Ni ratio = 500:1 to yield a polymer denoted POPT6. This polymer was expected to have a molecular weight around 135,000 g mol^{-1}. However, GPC experiments for the nonfractionated POPT6 indicated M_w = 50,000 g mol^{-1}. From the observation of the peak asymmetry and the presence of a shoulder toward low molar masses (between 5 × 10^3 and 10^4 g mol^{-1}), it is reasonable to assume that high molar mass material is retained during filtration before injection. Matric assisted-laser desorption/lonisation-time-of-flight spectrometry (MALDI-TOF) experiments were undertaken on POPTs, but trials remained unsuccessful even though a number of matrices were used (namely those based on sinapinic acid, 3,5-dimethoxy-4-hydroxybenzoic acid, 1,8,9-anthracene triol or 2,2′,5′,2″-terthiophene with and without a silver ion donor). We used both "sandwich" techniques and simple drop cast techniques to prepare the surfaces for ablation, as previously indicated.[47] This was probably due to the difficulty of ionizing carbocyclic-based structures. Finally, a GRIM based polymerization performed at 60 °C rather than at room temperature, yielded POPT7 with a GPC-indicated M_w = 39,000 g mol^{-1} and Đ = 1.7. The similar dispersity made it possible to compare it directly against samples POPT5 and POPT6.

Andersson et al.[35] showed that regioregular (94%) POPT could be obtained via the use of $FeCl_3$. An estimation of the degree of regioregularity of the POPT1 was made from the ratio of ^{1}H NMR integrals of signals at 2.73 and 2.62 ppm due to α-CH_2- groups on regular head-to-tail triads and on irregular head-to-head triads, respectively, as identified in Figure 4. POPT1 shows a similar degree of regioregularity (ca. 94%).

In contrast, and from comparable P3HTs, one would expect a much higher degree of regioregularity from POPT prepared using GRIM. Surprisingly, the ^{1}H NMR spectrum of POPT2 (Fig. 4) indicated a regioregularity (ca. 94%), when compared with the other samples shown in Table 1. It is understood that the GRIM polymerization "inserts" irregularities at one chain-end of the polymer,[18,19] and this material suffered from the presence of a high number of low molar mass chains. This confirmed that THF was not a good solvent in which to prepare POPT.

The remaining samples were prepared in DPE. Apart from variations in peak sizes, the ^{1}H and ^{13}C spectra of POPT3, POPT4, POPT5, and POPT7 were all very similar. Therefore, only the ^{1}H (Fig. 4) is shown. Again, one would expect reasonably high regioregularities but that of POPT4 (95%) is comparable with that of POPT1. Indeed, POPT3 and POPT5 were even lower at ∼90%. Although the value for POPT3 could be explained by a high content of short polymer chains in this sample (as indicated in Fig. 3) and Table 1, this is an unexpected value of regioregularity for the high-molecular weight sample POPT5. We attributed this to the use of a higher polymerization temperature (increased from 40 to 60 °C), used to obtain higher molar masses. This caused an

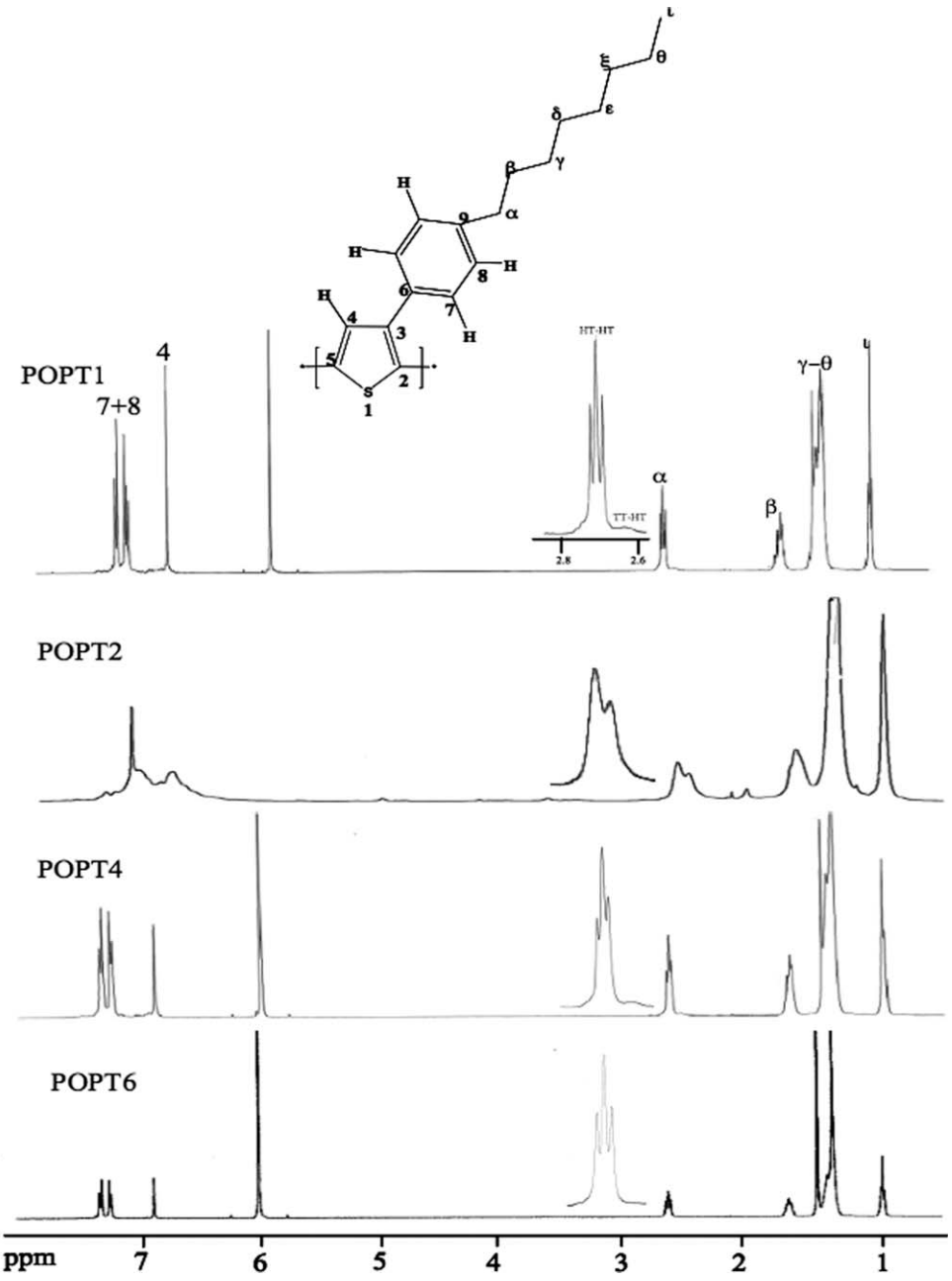

FIGURE 4 ^{1}H NMRs of POPT1, POPT4, and POPT6 ($C_2D_2Cl_4$, 100 °C) and POPT2 ($CDCl_3$, ambient temperature).

increased introduction of defects, probably due to secondary trans-metallation reactions.

Nevertheless, POPT6, prepared using a ratio monomer to Ni 500:1 and in DPE at 40 °C was expected to display, due to a low concentration of chain-ends, a higher degree of regioregularity. This was confirmed by ^{1}H NMR spectrum, where it is shown (Fig. 4) to be *quasi*-100% regioregular. This confirmed the role of the temperature during polymerization.

Further Characterizations—^{13}C NMR

A ^{13}C spectrum of a representative sample of (POPT4) is shown in the Supporting Information Figure 1, and the signals confirmed the expected structure. A 2D ^{1}H–^{13}C NMR HSQC spectrum of POPT4 was also performed (Supporting Information Fig. S2). In the region of the aliphatic protons, the methylene protons in α-position of the phenyl ring (triplet at 2.7 ppm) are correlated with the carbon peak at 36.1 ppm. The peak ^{1}H at 1.74 ppm, assigned to -CH_2-β, is correlated with carbon at 31.5 ppm and the peak ^{1}H at 1.45 ppm of the protons -CH_2-γ is correlated with carbon with 32.3 ppm. The three signals ^{13}C at 29.8, 29.7, and 29.6 ppm are correlated, respectively, with the protons H_δ, H_ε, and H_ξ. The signals ^{1}H due to -CH_2-θ and the methyl terminal groups are correlated with carbons resonating at 23.0 and 14.4 ppm, respectively. In the aromatic region, the ^{1}H singlet at 6.89 ppm assigned to H_4 is correlated with the peak ^{13}C at 130.3

ppm. The phenyl protons (H_7 and H_8), giving a double doublet in the ^1H spectrum, are correlated with the signals at 128.9 and 129.5 ppm in the ^{13}C spectrum. In Figure S2(a), the total decoupled ^{13}C NMR spectrum, the undecoupled ^{13}C spectrum and the ^{13}C NMR spectrum with selective decoupling of the α-CH_2- protons of carbons C_4, C_7, and C_8 are presented. These spectra allow to confirm the assignments of the peak due to the carbons C_7 and C_8. Indeed, the single signals at 128.9 ppm due to C_8 and the peak at 129.5 ppm due to C_7 observed in the decoupled spectrum become, respectively, a doublet of a quadruplet and a double-doublet in the undecoupled ^{13}C spectrum. The multiplicity of C_8 can be explained by two different couplings, with H_8 ($J^1 \sim 150$ Hz), and with $2H_\alpha$ and H_8' ($J^3 \sim 6$ Hz). In addition, the selective decoupling of the α-CH_2- protons only simplify the doublet-quadruplet in simple double-doublet, confirming that C_8 was coupled with the α-CH_2- protons. The double-doublet found for C_7 in the undecoupled spectrum is due to the couplings with H_7 ($J^1 \sim 150$ Hz) and with H_7' ($J^3 \sim 8$ Hz). It was noted that in the case of phenyl derivatives, a J^2(C-H) coupling constant could be estimated at 1 Hz and a J^3(C-H) at 8 Hz.[49] Thus, in the case of POPT, the J^2 (C-H) coupling constants of the carbons of the phenyl ring with their adjacent protons are too weak to be observed on the undecoupled ^{13}C spectrum. The Supporting Information Figure S2(b,c) present the decoupled and undecoupled ^{13}C spectra of the quaternary carbon region (C2, C3, C4, C6, and C9). The single signals at 131.4 and 134.8 ppm observed on the total decoupled spectrum, respectively, became a broad doublet with a coupling constant around 10 Hz and a doublet with a weak coupling constant (5 Hz) on the undecoupled spectrum. The first signal was allotted to C_2, as this carbon is coupled with H_4 with a large coupling constant J_3 (C_2-H_4) and the second peak corresponded to C_5 coupled with the H_4 with a weaker coupling constant J_2 (C_5-H_4). The peak at 133.6 ppm obtained as a triplet with a coupling constant of about 7 Hz, could be assigned to a carbon coupled with two protons with a J^3 coupling. This corresponds to C_9 supposed to be coupled with both protons H_7 with a J^3 C_9-H_3 coupling. From Figure 5(c), the assignments of carbons C_6 and C_3 can be made. The carbon C_6 is coupled, respectively, with both protons H_8 and with the proton H_4 with a similar J^3 (8–10 Hz) coupling, leading to an expected triplet in the undecoupled spectrum. The carbon C_3 is coupled with both protons H_7 ($J^3 \sim 8$–10 Hz) and proton H_4 ($J^2 \sim 2$-5 Hz), respectively. Thus, C_3 presents a narrower peak than that of C_6 in the undecoupled ^{13}C spectrum. Thus, the signal at 140.1 ppm can be attributed to carbon C_3 and the one at 143.1 ppm to C_6.

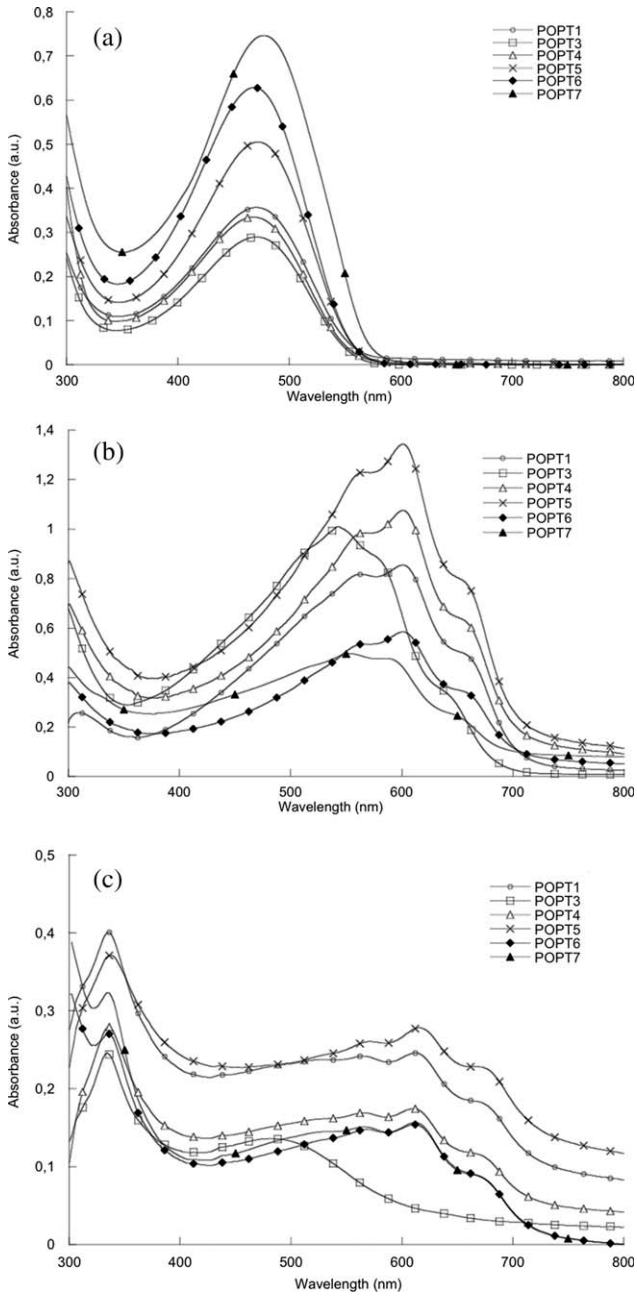

FIGURE 5 (a) Absorption UV-visible spectra of POPTs in solution in chloroform; (b) Absorption UV-visible spectra of annealed (120 °C for 5 min) POPTs on spin-coated films; and (c) Absorption UV-visible spectra of POPT:PCBM (1:1) blends on spin-coated films annealed at 120 °C for 5 min. Note the low λ_{max} for POPT3 due to its low molar mass.

Thermal Properties

The Supporting Information Figure S3 shows the TGA plots of the POPTs. Two clear steps can be seen in the thermal decomposition of the POPTs. The initial step started at about 280 °C for POPT1, POPT5, and POPT7 and about 300 °C for POPT3, POPT4, and POPT6. This first degradation was more rapid for POPT1, POPT5, and POPT7, closely followed by POPT3 and then POPT4 and POPT6. It is probable that this initial step was due to the loss of octyl chains, given that it yielded to a total loss of around 40% by weight. As to why the polymers exhibited different rates of loss is not clear. It is possible that the high concentration of high molar mass chains in POPT1 and POPT5 ($M_w > 50{,}000$ g mol^{-1}) and the bimodal distribution of molar mass led to a faster first degradation. In addition, the distribution of irregularities throughout its structure, rather than essentially at chain

TABLE 2 Electrochemical Properties of the POPTs

	p-Doping		*n*-Doping		
Polymer	E_{ox} (V)[a]	HOMO (eV)	E_{red} (V)	LUMO (eV)	E_g (eV)[b]
POPT1	0.52	−5.23	−1.73	−2.98	2.25
POPT4	0.66	−5.22	−1.65	−2.91	2.31

[a] Potential referred versus Fc/Fc^+ (see text).
[b] $E_g = (E_{ox} - E_{red})$.

ends as was the case for POPT3, may have enhanced instabilities. The second degradation process, which took place in a temperature range of 400–650 °C for POPT1, and POPT5 and 470–650 °C for POPT3, POPT4, POPT6, and POPT7 can be attributed to the polymer backbone degradation. However, from these TGA results, it is important to note that the thermal stability of the POPTs is adequate for the fabrication processes of photovoltaic devices.

POPT thermal properties were also studied by DSC to determine the nature of possible phase transitions. Heating and cooling cycles were performed using drop-cast thin films with a preliminary cycle to remove thermal histories. As the Supporting Information Figure S4 shows, no melting transitions were observed, a property in contrast to that of P3HT[50,51] and indicating a negligible concentration of crystallites. Nevertheless, the thermogram indicated that on cooling, there was a wide disorder-order transition with a peak at around 230 °C. Although this was a relatively large exothermic transition, it was difficult to assign it to a crystallization as the heating cycle showed no clear melting peak nor order–disorder transition for that matter. A weak T_g was detected at 160 °C, most likely due to in-chain rotations.

Optical and Electrochemical Properties

Once deposited on a platinum electrode, the electrochemical behavior of POPT1 and POPT4 were here considered representative of the two types of polymers in this series investigated by cyclic voltammetry (CV) in propylene carbonate with 0.1 M Bu_4NBF_4. Both polymers gave a reversible response in the positive potential range ascribed to a *p*-doping/dedoping process and an irreversible response in the negative potential range corresponding to irreversible *n*-doping process. The energy values of the lowest unoccupied molecular orbital (LUMO) and the highest occupied molecular orbital (HOMO) could thus be estimated for each polymer according to the following equations[52]: HOMO $= -(E_{ox} + 4.71)$ (eV), LUMO $= -(E_{red} + 4.71)$ (eV). The potential values referred to are versus the ferrocene/ferrocenium redox couple, Fc/Fc^+ ($E_{1/2}$ $Fc/Fc^+ = 0.15$ mV vs. Ag/10 mM $AgNO_3$). The redox data and energy levels are listed in Table 2. The HOMO and LUMO levels obtained for POPT1 and POPT4 are comparable. An average value of −5.2 eV for the HOMO level is obtained and is quite similar to that of P3HT.[53] However, the LUMO level is lower with an average value of −3 eV compared with −3.3 eV for P3HT. The values obtained with POPTs are in good agreement with the ones already reported.[38] We noticed a difference of the gap determined by CV (2.2 eV) and by optical absorption (1.76 eV), but this discrepancy has been observed elsewhere and is explained by considering that as the processes involved are not the same. In the case of optical transitions, there is no formation of free charge carriers, only a bound exciton. The formation of charge carriers will then require a higher energy. This argues that the optical bandgap is probably underestimated. In the case of CV, electrochemical doping processes are occurring.[54]

The UV-visible spectra of POPTs in chloroform solution are shown in Figure 5(a). All spectra present a maximum absorption in the visible region, around 470 nm, characteristic of the p–p^* transition of the dissolved polythiophene backbones. However, it is interesting to note that there is a slight shift due to the difference in molar masses. For photovoltaic applications, the absorbance of polymers in thin films, especially the absorbance in the visible region, is an important parameter. Solid-state absorption spectra of the POPT samples obtained after optimal thermal annealing are shown in Figure 5(b), and maximum values are recorded in Table 1. For all the samples, the absorption spectra present a red-shift compared with those obtained for P3HTs (λ_{max} around 550 nm).[43] Moreover, compared with the absorption spectra obtained from chloroform solutions, the maximum absorption wavelength of the thin films (spin-coated) are red-shifted by 100 to 150 nm, and an additional vibrational fine structure, tailing up to 800 nm, was observed. This indicates that the slightly higher degree of main chain conjugation and the presence of considerable inter-chain interactions between the polymer chains in the solid film are due to the presence of the pendent phenyl rings. It was shown that the phenyl group adds disorder to the polymer chain when considered in an isolated state, but on going to the solid state the chains become more planar.[55] An exception is POPT3, which did not contain any high molar mass material and exhibited a lower λ_{max} (540 nm). The optical band gaps deduced from the absorption edges of thin film spectra for all samples, around 1.7 eV, were lower than those found for P3HT (1.9 eV).

Figure 5(c) shows the absorption spectra of POPT-*blend*-PCBM films (1:1 by weight) prepared by spin coating from hot solutions in chlorobenzene (130 °C). The films were annealed at 120 °C for 5 min. The absorption bands are due to the polymer, except for the band at 340 nm which is characteristic of PCBM. POPT1, 4, 5, and 6 showed a slight increase in the wavelengths of the fine vibronic bands (from 10 to 20 nm) when going from films of the polymer alone to those with PCBM (as detailed in Table 1). It can be assumed that POPT, through the presence of pendent phenyl rings, is considerably more rigid than P3HT, and therefore any movement enhancing π-stacking is restricted in the solid state. However, the results seem to indicate that PCBM allows POPT a greater freedom of movement so that it can better self-organize to increase conjugation lengths and inter-chain interactions. Conversely, though in the case of POPT3 which contains low molar mass samples, the λ_{max} decreased in the presence of PCBM, and no vibrational fine structure was observed. This is an effect similar to that observed with

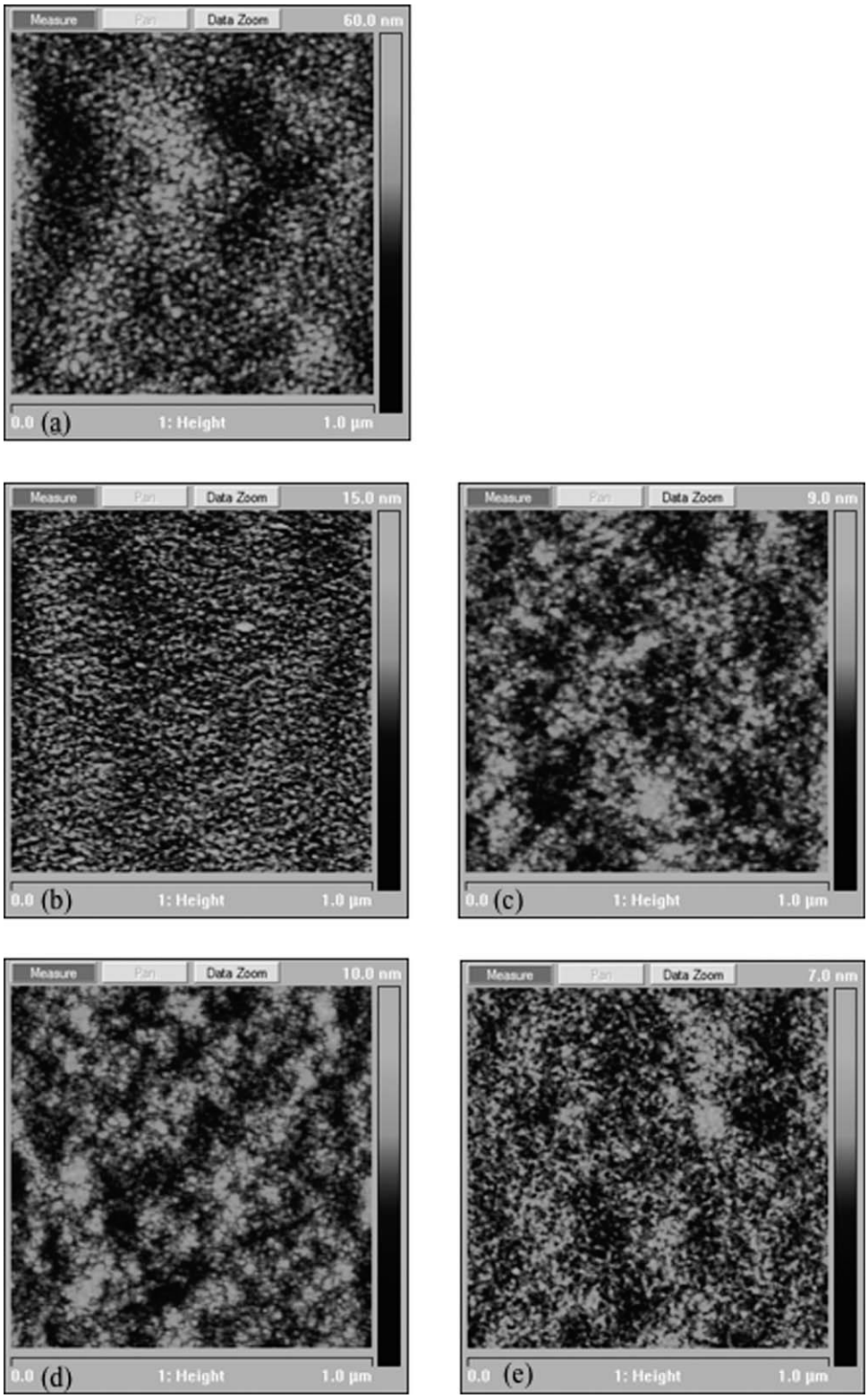

FIGURE 6 Height AFM images of spin coated thin films from chlorobenzene (a) POPT as deposited; (b) POPT:PCBM 1:1 (wt ratio) as deposited; (c) POPT:PCBM 1:1 5 min at 90 °C; (d) POPT:PCBM 1:1 5 min at 120 °C; and (e) POPT:PCBM 1:1 5 min at 150 °C.

P3HT, where close mixing of the two components is promoted by facile movement and the dislocation of the short polymer chains.[47]

Morphological and Photovoltaic Properties

The surface morphology of thin films was studied by AFM. First, thin films only based on POPT were studied to

TABLE 3 Photovoltaic Characteristics of ITO/PEDOT:PSS/POPT:PCBM (1:1)/LiF/Al Devices under AM 1.5 Illumination at an Irradiation of 100 mW cm^{-2} POPT:PCBM Blends Deposited from Chlorobenzene Solutions

POPT: PCBM (1:1)	Temperature (°C)	V_{oc} (V)	J_{sc} (mA cm^{-2})	*FF* (%)	PCE (%)
POPT1	25	0.63	3.05	36	0.69
	90	0.61	4.65	46	1.30
POPT3	25	0.54	1.28	28	0.19
	90	0.43	1.32	29	0.16
POPT4	25	0.67	3.26	40	0.87
	80	0.63	4.40	46	1.26
POPT5	25	0.62	4.02	40	1.01
	90	0.59	5.49	49	1.58
POPT6	25	0.57	4.69	42	1.14
	80	0.58	4.37	47	1.19
POPT7	25	0.61	4.75	44	1.29
	100	0.57	5.26	48	1.43

examine if this polymer could exhibit a fibrillar structure such as P3HT. The height image of a thin film as deposited from chlorobenzene is presented in Figure 6(a). It shows that there is no specific structuration, the film seemed to be amorphous.

The surface of thin films obtained from blends of POPT:PCBM (1:1 by weight) was followed with various thermal annealing processes [Fig. 6(c–f)]. These images showed that the roughness of the films is around 10 nm and that the morphology is dependent on the annealing temperature. In the case of P3HT, there is usually an increase in the fibrillar structure with thermal annealing. In the case of POPT, it is mainly the dispersion of PCBM in the polymer matrix that is modified. Indeed, as deposited, the blend is homogenous and seems amorphous. With a thermal annealing of 5 min at 90 °C, a slight phase segregation between polymer and PCBM was observed. By heating at 120 °C, the morphology remains virtually unchanged, but with a heating at 150 °C, the PCBM seems to be redispersed again in the polymer matrix. However, given that these are surface characterizations only, it is not possible to state anything about the underlying structure. There may have been a preference for the bulk-N_2 interface (these characterizations were performed under dry gas) by one component, or more likely, the lower molar mass parts of the relatively disperse polymer (POPT6) making their way to the surface at higher temperatures. Similar effects have been observed elsewhere in different systems.[56]

To study the photovoltaic performance of the POPTs, OPVs were fabricated with a structure ITO/PEDOT:PSS/POPT:PCBM (1:1)/LiF/Al. Preliminary results obtained on some POPTs without optimizations were previously reported.[40] The open-circuit voltage (V_{oc}), short circuit current density (J_{sc}), fill factor (*FF*), and power conversion efficiency (PCE) (PCE of the OPVs based on POPT1 and POPT3–7 (deposited from chlorobenzene solutions) under AM1.5 conditions (100 mW cm^{-2}), before and after heat treatments, are summarized in Table 3.

The performance parameters of devices from POPT1 to POPT7 increase with appropriate thermal treatments. A slight improvement in performances is observed after annealing POPT6 and POPT7. For the low molar mass sample (POPT3), no significant variation of the photovoltaic parameters are observed with annealing (V_{oc} = 0.55 V, J_{sc} = 1.28 mA cm^{-2}, PCE = 0.19%). But, the PCE and J_{sc} of POPT3 are reduced by approximately 80% compared POPTs with greater molar masses. Therefore, it can be assumed that the reduction of current density of POPT3 was probably due to the blue-shift in absorption spectrum [Fig. 5(c)] and its poor self assembly behavior with PCBM. The photovoltaic composites with low molar mass polymers have, in general, a reduced value of J_{sc}. Before heat treatment, the performance

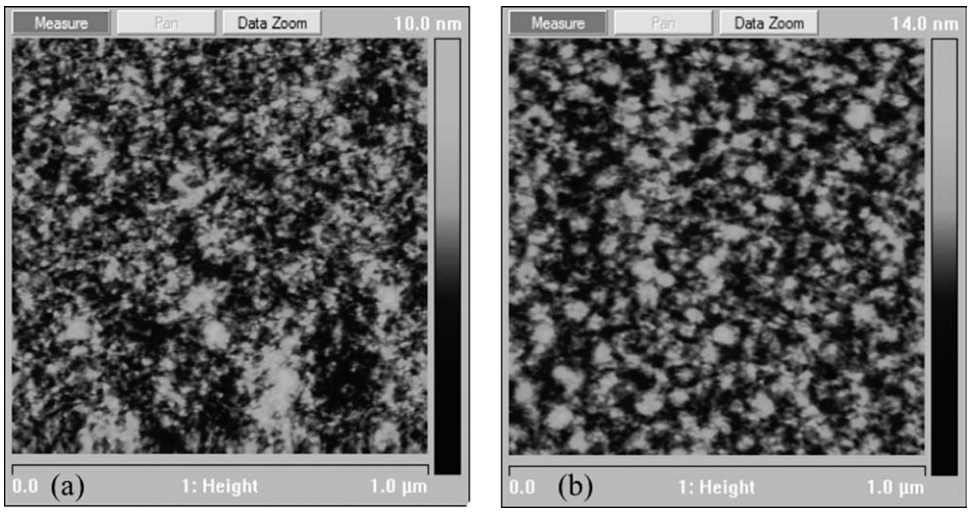

FIGURE 7 Height AFM images of POPT:PCBM cast from chlorobenzene: (a) POPT:PCBM 1:1.5 (wt ratio) and (b) POPT:PCBM 1:2 (wt ratio).

parameters of the devices increased on going from POPT5 (V_{oc} = 0.62 V, J_{sc} = 4.02 mA cm^{-2}, *FF* = 40%, PCE = 1.01%), to POPT6 (V_{oc} = 0.57 V, J_{sc} = 4.69 mA cm^{-2}, *FF* = 42%, PCE = 1.14%) and to POPT7 (V_{oc} = 0.61 V, J_{sc} = 4.75 mA cm^{-2}, *FF* = 44%, PCE = 1.29%). The difference between these three samples is mainly the molar mass that decreases from POPT5 to POPT7. It seems that greater annealing is necessary when using high molar mass samples, in agreement for results found for the comparable P3HT.[41] Although POPT6 presents a high degree of regioregularity (~100%) comparatively to POPT5 (91%). This indicates that the incorporation of a small amount of irregularities into the polymer backbone does not greatly affect the performances of the POPT solar cells.

After heat treatment, the devices based on samples that contain high molar mass polymers and a small amount of irregularities (POPT1, 4, and 5) exhibited a more pronounced improvement in the photovoltaic parameters (J_{sc}, *FF*, PCE), while V_{oc} remains nearly constant slightly above 0.60 V.

Generally, V_{oc} is related to the difference between the LUMO energy level of acceptor and the HOMO energy level of the conjugated polymer. Therefore, in the case of POPTs, V_{oc} attainable is in the same range of value as that of P3HT.[57] In contrast, the *PCE* reached a maximum value at 80 °C for POPT4 (1.26%), at 90 °C for POPT1 (1.3%), and at 90 °C for POPT5 (1.58%). The value of J_{sc} after annealing followed the order POPT5 (5.49 mA cm^{-1}), POPT1 (4.65 mA cm^{-1}), and POPT4 (4.40 mA cm^{-1}). The same extending annealing condition does not strongly affect the device performance of POPT6 (J_{sc} = 4.37 mA cm^{-2}, PCE = 1.19%). In the case of POPT7, the thermal annealing at 100 °C improved J_{sc} and *FF* the most, leading to an increase of PCE from 1.29% to 1.43%. It can be seen that while maximizing regioregularity in POPT may provide the best photovoltaic properties in the pristine material (without annealing), the best (annealed POPT5) photovoltaic performance is obtained with a POPT with a reduced degree of regioregularity. This is similar as a result to that demonstrated elsewhere for P3HT, where a reduced tendency to crystallize can result in a more stable interpenetration of polythiophene and PCBM-based phases.[58,59] As presented in Figure 3, POPT5 contained considerably higher molar mass polymer chains than POPT1, POPT4, and POPT6. However, the sample that contains high molar mass material (POPT5) exhibits a higher value of J_{sc} after heat treatment (J_{sc} = 5.5 mA cm^{-2}). This can indicate that the presence of high molar mass macromolecules ensures high charge mobilities and forms more thermally stable POPT:PCBM bulk-heterojunction devices.

Effect of POPT:PCBM Ratio

As AFM images showed a very homogeneous dispersion of PCBM in the polymer matrix for the blend 1:1 without annealing, which would tend to enhance charge-recombination rather than charge-transfer to the electrodes, higher PCBM contents were attempted. As shown in Figure 7, by increasing the ratio of PCBM compared with polymer, the phase separation was clearly modified. Indeed, by raising the ratio to 1:1.5, the PCBM was no-longer perfectly mixed with the polymer matrix and the phase separation was more clearly visible. This observation was confirmed in the case of POPT:PCBM 1:2, where the size of both domains was increased and estimated around 50 nm. This morphology would seem to be more appropriate for photovoltaic applications as there are phases which can transfer changes away from their point of formation.[60]

TABLE 4 Photovoltaic Characteristics of ITO/PEDOT:PSS/POPT:PCB/LiF/Al Devices under AM 1.5 Illumination at an Irradiation of 100 mW cm^{-2} POPT:PCBM Blends Deposited from *p*-xylene (Xyl) or Chlorobenzene (Clbz) Solutions, and for Different Ratios

	Solvent	POPT:PCBM	*T* (°C)	V_{oc} (V)	J_{sc} (mA cm^{-2})	*FF* (%)	PCE (%)
POPT5	Xyl	1:1	25	0.38	5.40	37	0.80
	Xyl	1:1	80	0.28	5.10	33	0.49
	Clbz	1:1	25	0.62	4.02	40	1.01
	Clbz	1:1	90	0.59	5.49	49	1.58
	Clbz	1:1.5	25	0.50	2.59	38	0.46
	Clbz	1:1.5	80	0.48	4.90	33	0.79
	Clbz	1:2	25	0.47	2.60	30	0.37
	Clbz	1:2	80	0.45	4.01	34	0.61
POPT7	Xyl	1:1	25	0.64	2.60	44	0.72
	Xyl	1:1	80	0.63	4.60	42	1.25
	Clbz	1:1	25	0.61	4.75	44	1.29
	Clbz	1:1	100	0.57	5.26	48	1.43
	Clbz	1:1.5	25	0.73	3.90	34	0.96
	Clbz	1:1.5	100	0.47	4.50	35	0.73
	Clbz	1:2	25	0.69	3.60	34	0.84
	Clbz	1:2	100	0.51	4.50	35	0.81

Ratios of 1:1.5 and 1:2 were chosen to test in solar devices for POPT5 and POPT7. The photovoltaic characteristics are summarized in Table 4.

The behavior of both polymers appeared to be very different with the increase of PCBM content. For POPT5, this had the effect to decrease the V_{oc} which is around 0.47 V whatever the ratio and the annealing temperature. Furthermore, J_{sc} increased with annealing leading to a higher PCE, as the *FF* was not greatly modified. In this series, the highest *PCE* (0.79%) was obtained with the ratio 1:1.5 after annealing at 80 °C. In the case of POPT7, the *PCE*s were higher on nonannealed devices with both tested ratios. And as for POPT5, the best result was obtained with the 1:1.5 ratio (0.96%). This *PCE* is higher than that obtained with POPT5 for the same ratio, due to a high value of V_{oc} (0.73 V). However, whatever the case, the usual 1:1 ratio remained the most suitable ratio for these two polymers as the *FF* obtained in this case was above 47%, compared with values around 34% for higher contents of PCBM.

Effect of Solvent for Deposition of the Active Layer

It has been shown that the morphology of the active layer is highly dependent on the solvent used for deposition.[61] *para-*

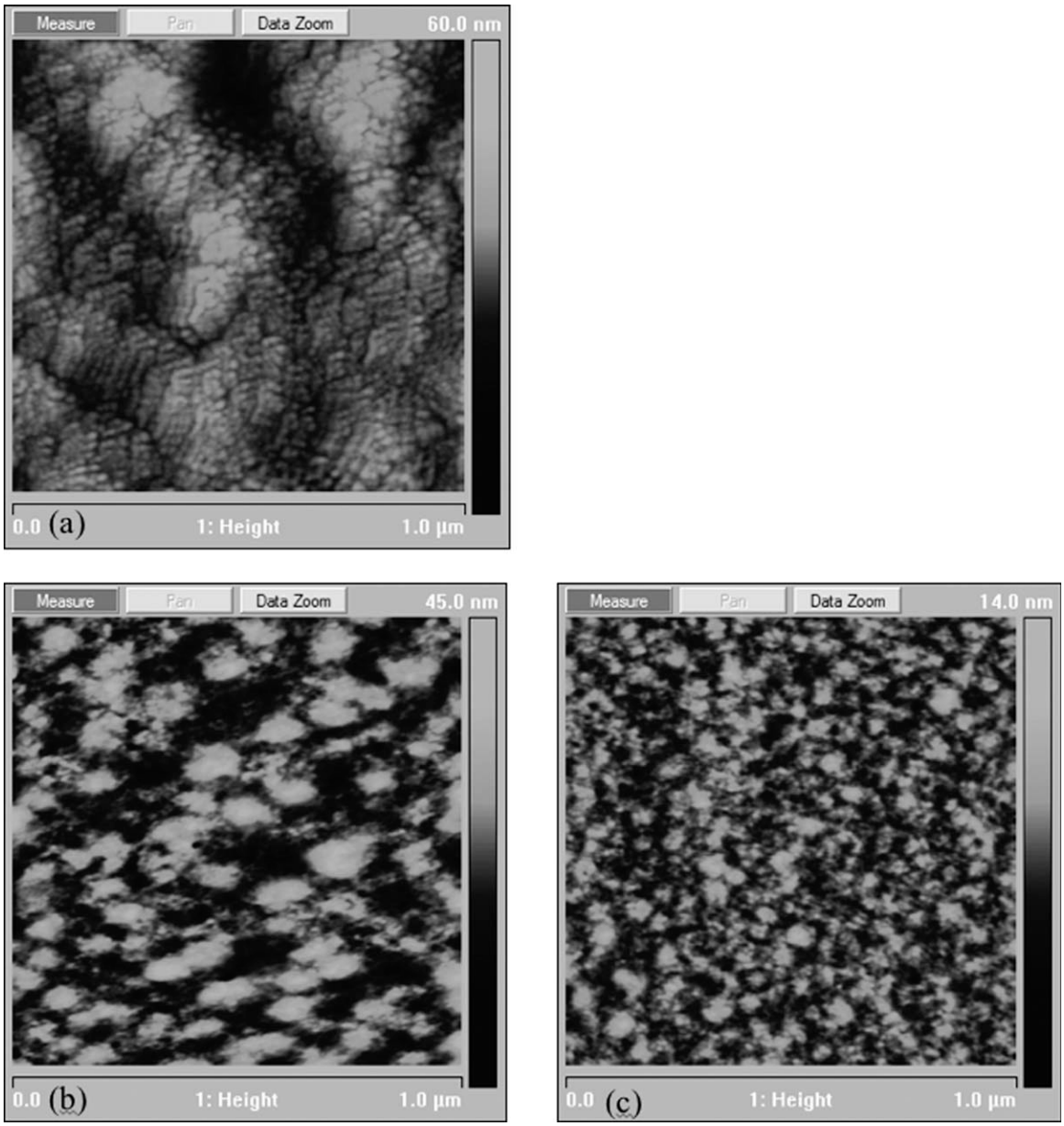

FIGURE 8 Height AFM images of: (a) POPT cast from *p*-xylene; (b) POPT:PCBM (1:1 wt) *p*-xylene; and (c) POPT/PCBM (1:2 wt) *p*-xylene.

Xylene is a poorer solvent than chlorobenzene for polythiophenes and can favor the formation of aggregates or fibrils in the case of P3HT.[62,63] With this in mind, *p*-xylene was used to prepare thin films of POPT and than POPT:PCBM blends. The AFM height image obtained in this case [Fig. 8(a)] showed a structuration of "platelets," probably induced by a crystallization obtained from solution. Two different POPT:PCBM ratios were tested. In the case of 1:1 ratio, a strong difference of morphology was observed between thin film prepared from chlorobenzene and the one prepared from *p*-xylene. In the latter, large domains of POPT were formed up to 100 nm, probably due to a phase separation even in solution. When doubling the PCBM content (1:2 ratio), the phase separation was reduced approximately by two, with an average domain size of 50 nm. One explanation could be that by increasing the content of PCBM, it disturbed the aggregation of POPT in *p*-xylene and thus diminished the domain size.

Tests in solar devices were performed for the 1:1 ratio for POPT5 and POPT7. In the case of POPT5, the V_{oc} was surprisingly low, 0.38 V at room temperature. All the parameters were decreased with annealing, leading to a decrease of PCE from 0.8% to 0.49%. In the case of POPT7, the V_{oc} was higher 0.64 V, but with a low J_{sc} (2.60 mA cm^{-2}), thus providing a PCE of 0.72%. An annealing at 80 °C did not change the V_{oc} but significantly increased the J_{sc} leading to a *PCE* of 1.25%. These results showed a clear difference of

parameters between POPT5 and POPT7 that could be explained by the difference of molar masses of the two polymers. Indeed, POPT5 (M_n = 65,000 g mol^{-1}, was probably poorly soluble in *p*-xylene, thus inducing aggregation in solution. This could affect the J_{sc} with a high content of charge recombination due to a large phase separation. Results with POPT7 were quite promising, even if the PCE remained lower with this solvent (1.25% after annealing) than that with chlorobenzene (1.58% after annealing). In all cases, POPT:PCBM blends prepared from chlorobenzene gave the best performances.

CONCLUSIONS

It has been shown that the GRIM chain-growth polymerization can be used to prepare POPTs with high molar masses by changing the usual solvent, THF, for DPE. Regioregularities obtained with this method are comparable with P3HTs and those obtained by oxidative polymerization using $FeCl_3$. As the GRIM reaction introduces mainly irregularities at chain ends, high molar mass polymers were targeted to diminish the irregularity content and to obtain improved solar cell performances. However, it was found that slightly reduced regioregularities had little impact on photovoltaic device characteristics. We have shown that the introduction of the phenyl ring on thiophene units improves the spectral absorption of the polythiophene toward the higher wavelengths with respect to P3HT and also improves the thermal stability. The bathochromic effect brought by the phenyl group is even increased in POPT:PCBM (1:1) blends with an extended absorption up to 750 nm. Electrochemical measurements have afforded the determination of energy levels, indicating that the HOMO level is quite similar to that of P3HTs. This can explain the relatively high values of V_{oc} obtained up to 0.67 V. Finally, the photovoltaic results obtained in solar cells with POPTs were encouraging with a PCE up to 1.58% with the higher molar mass POPT and with usual conditions (1:1 ratio and chlorobenzene as solvent). The limiting parameter is the J_{sc} which achieves at most 5.5 mA cm^{-2}. Changing conditions, such as component ratios and solvent, did not allow device improvements, even while AFM images indicated a positive change of morphology with an increase of the domain size. The solar cell results indicated that the molar masses of POPTs strongly affect the *PCE* and that each sample required independent optimization with respect to thermal annealing. The morphological study based on AFM images showed an unusual evolution of the morphology of the POPT:PCBM blend (1:1) on thermal annealing. After deposition, thin films were completely amorphous without phase separation, optimized thermal annealing promoted an interesting phase separation allowing an increase of photovoltaic parameters. But, in the case of POPTs, contrary to P3HTs, the PCBM seemed to be redispersed in the polymer matrix by continuing the increase in temperature.

The authors acknowledge Dr. Martial Billon and Dr Renaud Demadrille for the electrochemical characterizations of POPTs. This work was financially supported by the French National Agency of Research (ANR) through the project NANORGYSOL and the Conseil Régional d'Aquitaine.

REFERENCES AND NOTES

1 IPCC 4th Assessment Report: Climate Change. Available at: http://www.ipcc.ch/publications_and_data/publications_and_data_reports.shtml. Accessed July 5, **2011.**

2 Lewis, N. S.; Nocera, D. G. *Proc. Natl. Acad. Sci. U.S.A.* **2006,** *103*, 15729–15735.

3 Dennler, G.; Scharber, M. C.; Brabec, C. J. *Adv. Mater.* **2009,** *21*, 1323–1338.

4 Brabec, C. J.; Gowrisanker, S.; Halls, J. J. M.; Laird, D.; Jia, S. J.; Williams, S. P. *Adv. Mater.* **2010,** *22*, 3839–3856.

5 OPV's with efficiencies of ~ 10% "OE-A Roadmap for Organic and Printed Electronics" (3rd ed., 2009). Available at: http://www.vdma.org/wps/portal/Home/en. Accessed July 5, **2011.**

6 Kirova, N. *Polym. Int.* **2008,** *57*, 678–688.

7 Deibel, C.; Dyakonov, V. *Rep. Progr. Phys.* **2010,** *73*, 096401.

8 Clarke, T. M.; Durrant, J. R. *Chem. Rev.* **2010,** *110*, 6736–6767.

9 Gunes, S.; Neugebauer, H.; Sariciftci, N. S. *Chem. Rev.* **2007,** *107*, 1324–1338.

10 Thompson, B. C.; Frechet, J. M. J. *Angew. Chem. Int. Ed. Engl.* **2008,** *47*, 58–77.

11 Ma, W.; Yang, C.; Gong, X.; Lee, K.; Heeger, A. J. *Adv. Funct. Mater.* **2005,** *15*, 1617–1622.

12 Boudreault, P. L. T.; Najari, A.; Leclerc, M. *Chem. Mater.* **2011,** *23*, 456–469.

13 Cheng, Y. J.; Yang, S. H.; Hsu, C. S. *Chem. Rev.* **2009,** *109*, 5868–5923.

14 Zhan, X. W.; Zhu, D. B. *Polym. Chem.* **2010,** *1*, 409–419.

15 Liang, Y. Y.; Xu, Z.; Xia, J. B.; Tsai, S. T.; Wu, Y.; Li, G.; Ray, C.; Yu, L. P. *Adv. Mater.* **2010,** *22*, E135-E138.

16 Konarka. Available at: http://www.konarka.com/index.php/site/pressreleasedetail/konarkas_power_plastic_achieves_world_record_83_ efficiency_certification_fr. Accessed July 5, **2011.**

17 Solarmer. Available at: http://www.solarmer.com/index.php. Accessed July 5, **2011.**

18 Loewe, R. S.; Khersonsky, S. M.; McCullough, R. D. *Adv. Mater.* **1999,** *11*, 250–253.

19 Iovu, M. C.; Sheina, E. E.; Gil, R. R.; McCullough, R. D. *Macromolecules* **2005,** *38*, 8649–8656.

20 Yokozawa, T.; Yokoyama, A. *Chem. Rev.* **2009,** *109*, 5595–5619.

21 Osaka, I.; McCullough, R. D. *Acc. Chem. Res.* **2008,** *41*, 1202–1214.

22 Yokoyama, A.; Miyakoshi, R.; Yokozawa, T. *Macromolecules* **2004,** *37*, 1169–1171.

23 Sheina, E. E.; Liu, J.; Iova, M. C.; Laird, D. W.; McCullough, R. D. *Macromolecules* **2004,** *37*, 3526–3528.

24 Hiorns, R. C.; Khoukh, A.; Gourdet, B.; Dagron-Lartigau, C. *Polym. Int.* **2006,** *55*, 608–620.

25 Oshimizu, K.; Takahashi, A.; Rho, T.; Higashihara, T.; Ree, M.; Ueda, M. *Macromolecules* **2011,** *44*, 719–727.

26 Li, Y.; Zou, Y. *Adv. Mater.* **2008,** *20*, 2952–2958.

27 Zhou, E.; Tan, Z.; Yang, Y.; Huo, L.; Zou, Y.; Yang, C.; Li, Y. *Macromolecules* **2007,** *40*, 1831–1837.

28 Hou, J.; Tan, Z.; Yan, Y.; He, Y.; Yang, C.; Li, Y. *J. Am. Chem. Soc.* **2006,** *128*, 4911–4916.

29 Zhou, E.; Tan, Z.; Yang, C.; Li, Y. *Macromol. Rapid. Commun.* **2006,** *27*, 793–798.

30 Tu, G.; Bilge, A.; Adamczyk, S.; Forster, M.; Heiderhoff, R.; Balk, L. J.; Mühlbacher, D.; Morana, M.; Koppe, M.; Scharber, M. C.; Choulis, S. A.; Brabec, C. J.; Scherf, U. *Macromol. Rapid. Commun.* **2007,** *28*, 1781–1785.

31 Cravino, A. *Polym. Int.* **2007,** *56*, 943–956.

32 Ouhib, F.; Khoukh, A; Ledeuil, J.-B.; Martinez, H. Desbrières, J.; Dagron-Lartigau, C. *Macromolecules* **2008,** *41*, 9736–9743.

33 Tan, Z.; Hou, J.; He, Y.; Zhou, Y.; Yang, C. Li, Y. *Macromolecules* **2007,** *40*, 1868–1873.

34 Pei, Q. Järvinen, H.; Österholm, J. E.; Inganäs, O.; Laakso, J. *Macromolecules* **1992,** *25*, 4297–4301.

35 Andersson, M. R.; Selse, D.; Berggren, M.; Järvinen, H.; Hjertberg, T.; Inganäs, O.; Wennerström, O.; Österholm, J.-E. *Macromolecules* **1994,** *27*, 6503–6506.

36 Granstrom, M.; Petritsch, K.; Arias, A. C.; Lux, A.; Andersson, M. R.; Friend, R. H. *Nature* **1998,** *395*, 257–260.

37 Holcombe, T. W.; Woo, C. H.; Kavulak, D. F. J.; Thompson, B. C.; Fréchet, J. M. J. *J. Am. Chem. Soc.* **2009,** *131*, 14160–14161.

38 Woo, C. H.; Holcombe, T. W.; Unruh, D. A.; Sellinger, A.; Fréchet, J. M. *J. Chem. Mater.* **2010,** *22*, 1673–1679.

39 Cho, C.-H.; Kang, H.; Kang, T. E.; Cho, H.-H.; Yoon, S. C.; Jeon, M.-K.; Kim, B. J. *Chem. Commun.* **2011,** *47*, 3577–3579.

40 Ouhib, F.; Hiorns, R. C.; Bailly, S.; de Bettignies, R.; Khoukh, A.; Preud'homme, H.; Desbrières, J.; Dagron-Lartigau, C. *Eur. Phys. J. Appl. Phys.* **2007,** *37*, 343–346.

41 Ouhib, F.; Hiorns, R. C.; de Bettignies, R.; Bailly, S.; Desbrières, J.; Dagron-Lartigau, C. *Thin Solid Films* **2008,** *516*, 7199–7204.

42 Venkatachalapathy, C.; Pitchumani, K. *Tetrahedron* **1993,** *53*, 2581–2586.

43 Järvinen, H.; Laakso, J.; Taka, T.; Österholm, J. E.; Pei, Q.; Inganäs, O. *Synth. Met.* **1993,** *55–57,* 1260–1265.

44 Tamao, K.; Kodama, S.; Nakjima, I.; Kumada, M. *Tetrahedron* **1982,** *38*, 3347–3354.

45 Aasmundtveit, K. E.; Samuelsen, E. J.; Mammo, W.; Svensson, M.; Andersson, M. R.; Pettersson, L. A. A.; Inganäs, O. *Macromolecules* **2000,** *33*, 5481–5489.

46 Kline, R. J.; McGehee, M. D.; Kadnikova, E. N.; Liu, J.; Fréchet, J. M. J.; Toney, M. F. *Macromolecules* **2005,** *38*, 3312.

47 Hiorns, R. C.; de Bettignies, R.; Leroy, J.; Baily, S.; Firon, M.; Sentein, C.; Khoukh, A.; Preud'homme, H.; Dagron-Lartigau, C. *Adv. Funct. Mater.* **2006,** *16*, 2263–2273.

48 Liu, J.; Loewe, R. S.; McCullough, R. D. *Macromolecules* **1999,** *32*, 5777–5785.

49 Levy, G. C.; Nelson, G. L. Carbon 13 Nuclear Magnetic Resonance for Organic Chemists; Wiley: New York, **1972.**

50 Cugola, R.; Giovanella, U.; Di Gianvincenzo, P.; Bertini, F.; Catellani, M.; Luzzati, S. *Thin Solid Films* **2006,** *511–512*, 489–493.

51 Ze, A.; Saphioannikova, M.; Neher, D.; Grenzer, J.; Grigorian, S.; Pietsch, U.; Asawapirom, U.; Janietz, S.; Scherf, U.; Lieberwirth, I.; Wegner, G. *Macromolecules* **2006,** *39*, 2162–2171.

52 Sun, Q. J.; Wang, H. Q.; Yang, C. H.; Li, Y. F. *J. Mater. Chem.* **2003,** *13*, 800–806.

53 Ong, B.; Wu, Y.; Jiang, L.; Liu, P.; Murti, K. *Synth. Met.* **2004,** *142*, 49–52.

54 Johansson, T.; Mammo, W.; Svensson, M.; Andersson, M. R.; Inganäs, O. *J. Mater. Chem.* **2003,** *13*, 1316–1323.

55 Dkhissi, A.; Ouhib, F.; Iratçabal, P.; Pouchan, C.; Hiorns, R. C.; Dagron-Lartigau, C. To be submitted for publication.

56 Hiorns, R. C.; Cloutet, E.; Ibarboure, E.; Vignau, L.; Lemaitre, N.; Guillerez, S.; Absalon, C.; Cramail, H. *Macromolecules* **2009,** *42*, 3549.

57 Scharber, M. C.; Mühlbacher, D.; Koppe, M.; Denk, P.; Waldauf, C.; Heeger, A. J.; Brabec, C. J. *Adv. Mater.* **2006,** *18*, 789–794.

58 Sivula, K.; Luscombe, C. K.; Thompson, B. C.; Fréchet, J. M. J. *J. Am. Chem. Soc.* **2006,** *128*, 13988–13989.

59 Woo, C. H.; Thompson, B. C.; Kim, B. J.; Toney, M. F.; Fréchet, J. M. *J. Am. Chem. Soc.* **2008,** *130*, 16324–16329.

60 Yang, X.; Loos, J.; Veenstra, S. C.; Verhees, W. J. H.; Wienk, M. M.; Kroon, J. M.; Michels, M. A. J.; Janssen, R. A. J. *Nano Lett.* **2005,** *5*, 579–583.

61 Hoppe, H.; Sariciftci, N. S. *J. Mater. Chem.* **2006,** *16*, 45–61.

62 Berson, S.; De Bettignies, R.; Bailly, S.; Guillerez, S. *Adv. Funct. Mater.* **2007,** *17*, 1377–1384.

63 Bertho, S.; Oosterbaan, W. D.; Vrindts, D.; D'Haen, J.; Cleij, T. J.; Lutsen, L.; Manca, J.; Vanderzande, D. *Org. Electron.* **2009,** *10*, 1248–1251.